ACS Sustainable Chemistry & Engineering

Research Article

Cite This: ACS Sustainable Chem. Eng. 2019, 7, 3301−3308

pubs.acs.org/journal/ascecg

# Chemical Liquid Deposition Modified 4A Zeolite as a Size-Selective Adsorbent for Methane Upgrading, $CO_2$ Capture and Air Separation

Yiren Wang and Ralph T. Yang*

Department of Chemical Engineering, University of Michigan, Ann Arbor, Michigan 48109, United States

Supporting Information

**ABSTRACT:** Chemical liquid deposition (CLD) modified 4A zeolite is developed as a size selective sorbent at 0.01 nm resolution for gas separation. The silica layer formed by CLD modification is located on the external surface of 4A zeolite, resulting in reduced pore apertures while not altering internal cavities. With controllable pore aperture sizes, the sorbents were able to selectively adsorb carbon dioxide, hydrogen sulfide and oxygen while excluding methane, nitrogen and argon, for application to methane upgrading from biogas, $CO_2$ capture and as an oxygen-selective sorbent for energy-saving air separation. The optimized CLD modified 4A zeolite samples achieved a $CO_2/CH_4$ (pure-component) selectivity as high as 76, a $CO_2/N_2$ selectivity of 44, an $O_2/N_2$ selectivity of 1.6 and an $O_2$/Ar selectivity of 2, while preserving high adsorption capacities for the targeted molecules. It was shown that the hydroxyl groups on zeolites were essential in the CLD mechanism and that the deposited CLD layer offered no diffusion resistance to the small molecules studied. The success of pore confinement provides a strategy for the development of efficient and scalable sorbents for size-selective separations.

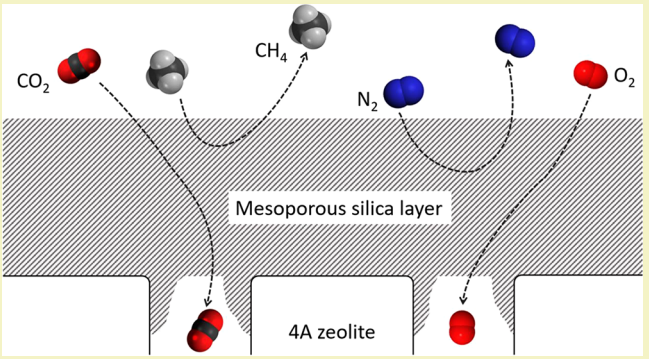


**KEYWORDS:** *CLD-4A, Biogas separation, $CO_2$ capture, $O_2$-selective sorbent for air separation*

## INTRODUCTION

Zeolites are crystalline aluminosilicates commonly used as sorbents and catalysts.[1] With tunable pore sizes and cavities of molecular dimensions, zeolites can be used in molecular-sieving separations, which is accomplished by size exclusion. An example is the use of zeolite 3A as a desiccant for petroleum cracking gas. The effective aperture size of 3A zeolite is 3 Å, which admits water and excludes all hydrocarbons.

The pore size of zeolites and their adsorptive properties can be tailored by changing the crystal structure and modifying the external surface.[1−8] Changing zeolite's crystal structures is effective for adjusting pore size and commonly used techniques include ion exchange,[2] element substitution and selective removal in the zeolite framework.[9,10] The modification of the external surface of zeolites allows for a refined alteration of their pore entrance sizes and also the possibility of changing the pore entrance sizes without affecting the internal structure. Yu et al. reported using molecular layer deposition (MLD) to place an ultrathin porous film on nanoparticles, such as depositing a porous alumina coating on the surface of 5A zeolite.[5,11] The misalignment between the pores of alumina coating and the 5A zeolite pores adjusted the aperture size of 5A zeolite, which made it useful for separating small organic molecules by diameter.[5] Niwa et al. used chemical vapor deposition (CVD) to deposit a silica layer on mordenite, thereby reducing the pore entrance sizes at 0.1 nm level.[3] It is expected that the silica layer will only be deposited on the external surface and pore opening region of the zeolite crystals as the molecular diameter of tetramethyl orthosilicate, the $SiO_2$ precursor, is larger than the pore size of mordenite.[3,12] This approach of modification of pore aperture size by external surface deposition was subsequently extended to chemical liquid deposition (CLD). Compared with CVD, CLD is simpler to control, and is thus more easily scalable as well as being amenable to finer tuning.[6,12] CLD modification is mostly used to improve catalyst performance. Recently, a few CLD modified zeolites have been used as sorbents. Gao et al. used CLD modified ZSM-5 in the adsorption separation of isomers of disubstituted benzene, such as *m*-xylene/*p*-xylene and *m*-cresol/*p*-cresol.[6] Shen et al. reported applying CLD modified ZSM-5 in selective adsorption removal of dimethyl disulfide from methyl *tert*-butyl ether.[7] CLD modified 5A zeolite was reported by Liu et al., who used this material to separate refrigerant mixtures consisting of R125 and R143a.[8]

Difficult separations that require a resolution in molecular size difference of 0.01 nm can be a major challenge in developing renewable energy resources and technologies. These include the upgrading of methane ($CH_4$) from biogas by removing carbon dioxide ($CO_2$) and hydrogen sulfide

Received: October 16, 2018
Revised: December 6, 2018
Published: January 4, 2019

Downloaded by UNIV OF MICHIGAN ANN ARBOR at 11:58:30:272 on June 03, 2019
from https://pubs.acs.org/doi/10.1021/acssuschemeng.8b05339.


© 2019 American Chemical Society

DOI: 10.1021/acssuschemeng.8b05339
ACS Sustainable Chem. Eng. 2019, 7, 3301−3308

($H_2S$), postcombustion $CO_2$ capture from flue gases (containing mostly $N_2$), and $O_2$ selective adsorption separation from air. Biogas such as landfill gas is produced from anaerobic digestion or degradation of organic material and landfill.[13] It contains approximately 50% of $CH_4$, 50% of $CO_2$ and $H_2S$ ranging from a few ppm to 0.4%.[14] The separated methane can be used as a renewable substitute for fossil fuels. The atmospheric $CO_2$ is the main cause for global warming.[15,16] Since the majority of emitted $CO_2$ is generated by the combustion of fossil fuels, separation of $CO_2$ from flue gas and $CO_2$ storage is a direct route for mitigating $CO_2$ emissions and ensuring environmental sustainability. Both biogas upgrading ($CO_2/CH_4$ separation, $H_2S/CH_4$ separation) and $CO_2$ capture ($CO_2/N_2$ separation) can be achieved through pressure swing adsorption (PSA) process or temperature swing adsorption (TSA) process.[16−19] At the heart of the process is a good sorbent with high capacity and high selectivity. In recent years, considerable effort has been made to develop efficient sorbents for $CO_2/CH_4$ and $CO_2/N_2$ separations, such as amine-grafted silica,[20−22] amine-impregnated silica,[23,24] amine-grafted zeolites,[25] cation-exchanged zeolites,[26−28] surface functionalized carbon,[29,30] modified clays materials[31] and metal−organic frameworks.[32−34] Another gas separation technique that is relevant for the reduction of $CO_2$ emissions is $O_2$ enrichment from air. High purity oxygen is a key component in oxy-combustion technology which can increase the combustion efficiency and reduce $CO_2$ emission.[35] Air separation is an important industry because $N_2$ and $O_2$ are, respectively, the second and third largest human-made chemicals. Air separation is accomplished by cryogenic distillation and PSA process using $N_2$-selective zeolites, both are energy intensive. Development of $O_2$-selective sorbent would lead to low-energy air separation, as explained further below. The polarizabilities of $N_2$, $O_2$ and Ar (main components of air with 78% $N_2$, 21% $O_2$ and 1% Ar) are nearly the same, resulting in similar adsorbed amounts on all sorbents except zeolites. Zeolites are used for air separation due to the interactions between the zeolitic cations and the stronger quadruple moment of $N_2$ compared with that of $O_2$. It is highly desirable to have an $O_2$ selective (over $N_2$) sorbent because much less work would be needed to achieve air separation by using such a sorbent.[1] Currently, the best commercial sorbent for air separation is the $N_2$ selective Li-LSX (low silica X, Si/Al = 1).[1] Most sorbents mentioned above are operated via chemisorption interactions or weak physisorption. In this work, we are interested in developing a new sorbent to separate $CO_2/CH_4$, $H_2S/CH_4$, $CO_2/N_2$ and $O_2/N_2$ by size exclusion. It is noted that in developing sorbents for these separations, effects of moisture is not considered as a primary factor. This is because, in commercial operations, moisture is removed effectively by using a layer of desiccant known as guard bed, e.g., in PSA separation of air using zeolites.

Herein we showed that the sizes of the pore mouths of Na-LTA zeolite (4A zeolite) could be reduced and tuned by a judicious CLD process. Single gas ($CO_2$, $CH_4$, $N_2$, $O_2$, Ar) adsorption isotherms of CLD modified samples were measured at 298 K. The high adsorption selectivities and capacities observed on the CLD modified 4A zeolite samples showed its potential for separations by size-selective adsorption.

## EXPERIMENTAL SECTION

**CLD Modification of 4A Zeolite.** Typically, the commercially available 4A zeolite powder (1 g) was dispersed in cyclohexane (3 mL). Then a predetermined amount of silicon tetrachloride, which corresponds to the overall loading of 16 wt % $SiO_2$, 23 wt % $SiO_2$ and 27 wt % $SiO_2$, was introduced into the mixture of 4A zeolite and cyclohexane. The CLD modification process was carried out for 4 h under stirring at ambient temperature. The mixture was dried at 373 K before being calcined at 773 K for 4 h in air. The samples are referred to as $16SiO_2$-CLD-4A, $23SiO_2$-CLD-4A and $27SiO_2$-CLD-4A.

**Adsorption Measurement and Characterization.** Adsorption isotherms of carbon dioxide, methane, nitrogen, oxygen and argon were measured with a static volumetric instrument, Micromeritics ASAP 2020. $CO_2$ adsorption isotherms were measured at 273 and 298 K. $N_2$ adsorption/desorption isotherms were measured at 77 K. Other pure gas isotherms were acquired at 298 K. Prior to each measurement, the samples were degassed at 623 K for 4 h to remove adsorbed moisture and gases. $H_2S$ adsorption isotherm was measured using a Shimadzu TGA-50H thermogravimetric analyzer at different $H_2S$ concentrations. Transmission electron microscopy (TEM) images were taken by a JEOL 2010F scanning transmission electron microscope. Thermogravimetric analysis (TGA) was performed on a Shimadzu TGA-50H apparatus. To determine the amount of hydroxyl groups on zeolites, the samples were heated from ambient temperature to 800 °C at a heating rate of 10 °C/min under a helium flow of 50 mL/min.

**Pure-Component Selectivity Determination.** The pure-component selectivity is used to evaluate the selectivity of different sorbents. The pure-component selectivity of gas 1 over gas 2 for a certain sorbent is defined as

$$\text{Pure-component selectivity} = \frac{Q_{\text{c-gas1}}}{Q_{\text{c-gas2}}} \quad (1)$$

Where $Q_{\text{c-gas1}}$ is the capacity of gas 1 at 760 Torr and 298 K, $Q_{\text{c-gas2}}$ is the capacity of gas 2 at 760 Torr and 298 K. Because the concentration of $CO_2$ in flue gas is approximately 15% and that of $N_2$ is about 80%, the corresponding pure-component selectivity for carbon capture sorbents is calculated by using $CO_2$ capacity at 0.15 atm and $N_2$ capacity at 0.8 atm.

## RESULTS AND DISCUSSION

The commercial 4A zeolite has an effective aperture size of 0.38 nm, which is close to that of many gases with kinetic diameters in the 0.3−0.4 nm range ($CO_2$, 0.33 nm; $O_2$, 0.35 nm; $H_2S$, 0.36 nm; $N_2$, 0.364 nm; $CH_4$, 0.38 nm). This makes 4A zeolite a good starting material to be modified to realize size-selective adsorption separations. In this work, silicon tetrachloride ($SiCl_4$) is used as deposition agent for CLD modification process. As the molecular size of $SiCl_4$ (0.71 nm) is bigger than the 4A zeolite aperture, the modification is expected to occur on the external surface of 4A zeolite.

The TEM images of the $27SiO_2$-CLD-4A sample are shown in Figure 1. After calcination, a silica layer with a thickness of 50−70 nm was deposited on the 4A zeolite crystals. Both the 4A zeolite and silica are stable commercial adsorbents. Therefore, it may be concluded that this new composite adsorbent is stable for adsorption process.

The textural properties of 4A zeolite and CLD modified 4A zeolite were investigated by $CO_2$ adsorption at 273 K and $N_2$ adsorption−desorption at 77K. Since there is no NLDFT kernel for $CO_2$-zeolite/silica at 273 K, the $CO_2$ adsorption isotherms measured at 273 K were analyzed by using the nonlocal density functional (NLDFT) models for carbon dioxide on slit-pore carbon to calculate the pore size distribution. As shown in Figure 2, the 4A zeolite exhibits uniform distribution of pores around 0.35 nm, smaller than its effective aperture size (0.38 nm). The small difference of 0.03


DOI: 10.1021/acssuschemeng.8b05339
ACS Sustainable Chem. Eng. 2019, 7, 3301−3308

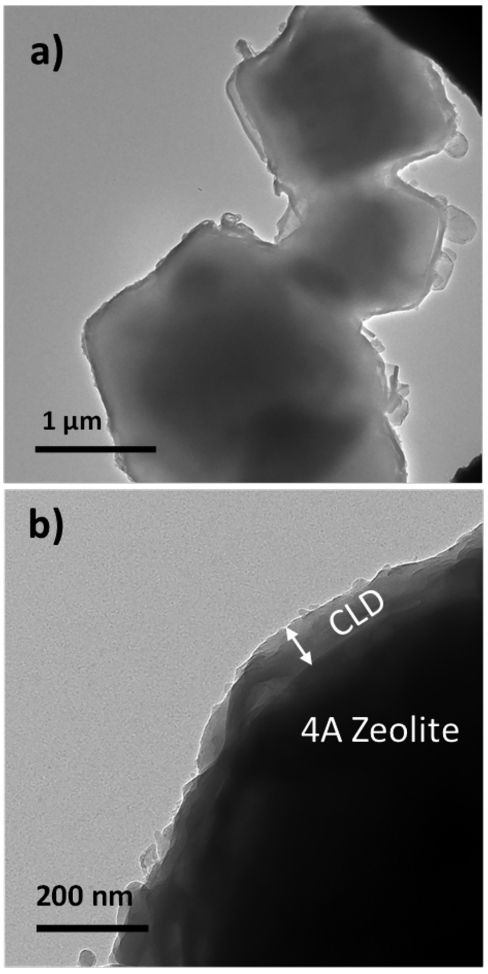


**Figure 1.** TEM images of $27SiO_2$-CLD-4A

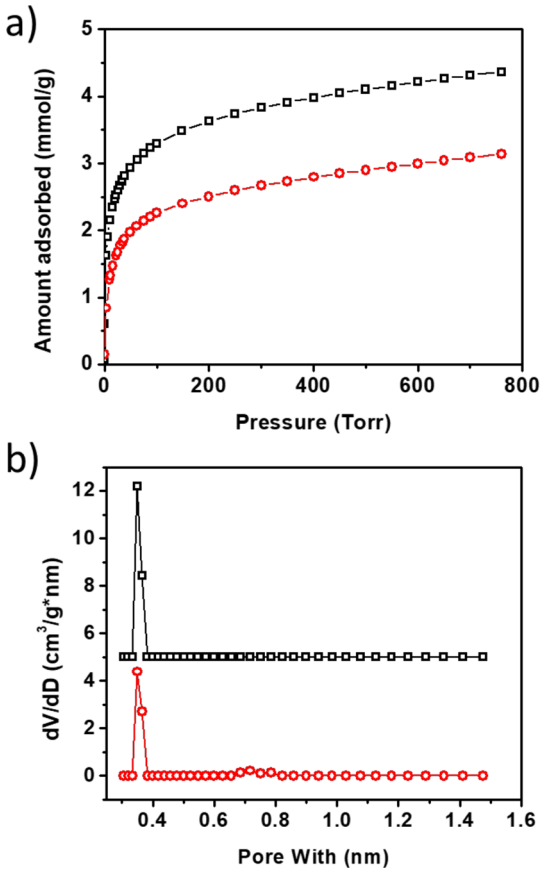


**Figure 2.** $CO_2$ isotherm (a) and pore size distribution (b) of 4A zeolite (□) and $27SiO_2$-CLD-4A (○) at 273 K; pore size distribution of 4A zeolite was offset by 5 $cm^3/(g{\cdot}nm)$ for clarity; the pore volume distribution is calculated from $CO_2$ adsorption isotherm at 273 K using NLDFT $CO_2$-carbon equilibrium transition kernel at 273 K based on a slit-pore model.

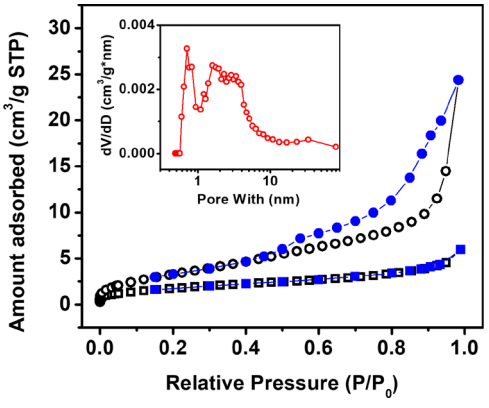


**Figure 3.** $N_2$ adsorption/desorption isotherms of 4A zeolite (□) and $27SiO_2$-CLD-4A (○) at 77 K (open symbols, adsorption; closed symbols, desorption) BJH pore size distribution (inset) of $27SiO_2$-CLD-4A (○).

nm in the measured pore size may be attributed to the fact that the NLDFT model used is developed based on porous carbons. The $27SiO_2$-CLD-4A sample contains the same micropores of 0.35 nm and some larger pores with the size around 0.7−0.8 nm, which is introduced by the silica layer, as a result of air calcination of the deposited layer of $SiCl_4$ at 773 K for 4 h. The primary pore size of 4A zeolite did not change after CLD process suggesting that the silica layer stayed only on the external surface and did not enter the internal pores of 4A zeolite. The $27SiO_2$-CLD-4A sample can be seen as a composite sorbent consisting of 73 wt % 4A zeolite and 27 wt % $SiO_2$. The $CO_2$ capacity of the zeolite 4A sample was 4.3 mmol/g at 760 Torr. The amount of $CO_2$ adsorbed on silica gel at 760 Torr and 273 K was 1.5 mmol/g according to literature.[36] Theoretically, the amount of $CO_2$ adsorbed on the $27SiO_2$-CLD-4A sample should be 3.5 mmol/g, which is a combination of the capacity of 4A zeolite and silica layer. The measured $CO_2$ capacity of the $27SiO_2$−CLD-4A sample (3.1 mmol/g) is slightly lower than its theoretical capacity, indicating that some of the pores are blocked or smaller than the diameter of $CO_2$ while the majority of the pores are accessible for $CO_2$ molecules. In addition, the deposited CLD silica layer is expected to adsorb less $CO_2$ than that on silica gel.

Figure 3 shows the $N_2$ adsorption−desorption isotherms of 4A zeolite and the $27SiO_2$-CLD-4A sample. The adsorbed amounts of $N_2$ on both samples were low due to the slow diffusion of $N_2$ at 77K and the short adsorption equilibrium time setting for each measurement point. Brunauer−Emmett−Teller (BET) surface area analysis showed that the BET specific surface area of 4A zeolite was 6.6 $m^2/g$ and that of the $27SiO_2$-CLD-4A sample was 12.9 $m^2/g$. This indicated that the BET specific surface area of the silica layer was 23.3 $m^2/g$. According to the IUPAC classification,[37] the adsorption



DOI: 10.1021/acssuschemeng.8b05339
ACS Sustainable Chem. Eng. 2019, 7, 3301−3308

isotherm of 4A zeolite exhibited the adsorption curve of type I with no hysteresis loop, which means 4A zeolite did not contain mesopores. The $N_2$ adsorption isotherm of the $27SiO_2$-CLD-4A sample corresponds to a type IV isotherm with a type H2 hysteresis loop, demonstrating the presence of mesopores in the CLD modified 4A zeolite. Furthermore, the pore size distribution of the $27SiO_2$-CLD-4A sample calculated by Barrett–Joyner–Halenda (BJH) method indicates that the sample contains pores of around 0.7 nm and 1.6–4.0 nm, which is in good accordance with the pore size distribution measured by $CO_2$ adsorption isotherms at 273 K. These larger pores in the $27SiO_2$-CLD-4A sample are attributed to the silica layer deposited on the 4A zeolite surface. Thus, the outer silica layer provides free paths for diffusion for the gas molecules included in this study.

The separation of $CO_2/CH_4$ is industrially important in biogas upgrading and natural gas processing. The adsorption isotherms of pure $CO_2$ and methane on 4A zeolite and $27SiO_2$-CLD-4A sample at 298 K are compared in Figure 4. After CLD

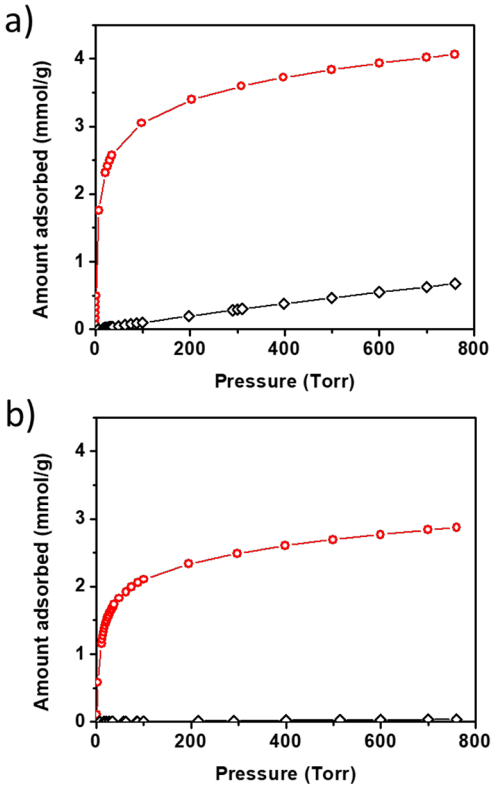


**Figure 4.** $CO_2$ (○) and methane (◇) isotherms on (a) 4A zeolite and (b) $27SiO_2$-CLD-4A at 298 K.

modification, the amount of methane adsorbed (at 760 Torr) on 4A zeolite decreased from 0.7 to 0.04 mmol/g, which means the majority of methane molecules were blocked from entering the 4A zeolite pores. The remaining methane adsorbed on the $27SiO_2$-CLD-4A sample could be the methane adsorbed on the silica layer. The pure-component selectivity calculated from the capacities of $CO_2$ and $CH_4$ was improved significantly from 6 to 76, indicating that the slightly bigger methane molecules (kinetic diameter of 0.38 nm) were effectively excluded. The $CO_2$ capacity of the $27SiO_2$-CLD-4A sample at 298 K and 760 Torr was 2.9 mmol/g. The high $CO_2$ adsorption capacity and $CO_2/CH_4$ selectivity of $27SiO_2$-CLD-4A demonstrated its great potential as a highly selective sorbent for $CO_2/CH_4$ separation. $H_2S$ is another gas that needs to be removed from biogas and natural gas.[14,38] Besides its toxicity, $H_2S$ leads to the corrosion of pipelines and is a hazardous compound that causes acid rain when oxidized in the atmosphere. The adsorption isotherms of low concentration $H_2S$ and pure $CH_4$ on $23SiO_2$-CLD-4A sample at 298 K are compared in Figure 5a. The concentration of $H_2S$ was

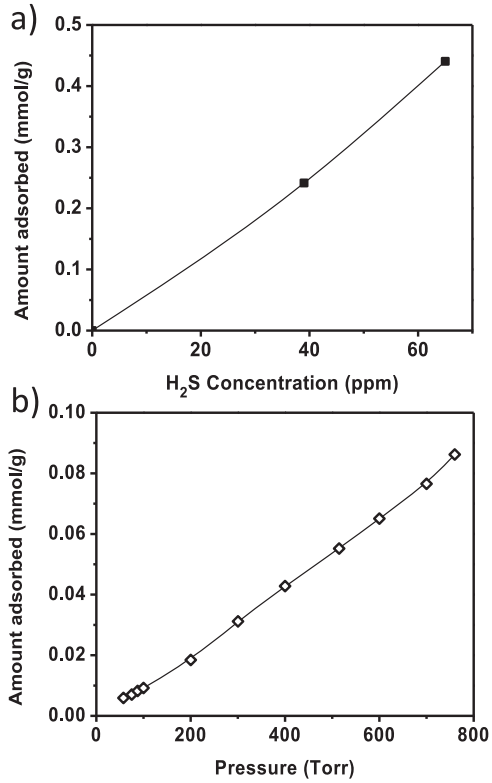


**Figure 5.** $H_2S$ (a) and methane (b) isotherms on $23SiO_2$-CLD-4A at 298 K.

increased every 60 min (for time saving purpose) to acquire the $H_2S$ isotherm. At 760 Torr, most $CH_4$ molecules are blocked to enter the 4A zeolite pores, resulting in less than 0.09 mmol/g of $CH_4$ adsorbed on $23SiO_2$-CLD-4A. This is much smaller than the amount of $H_2S$ adsorbed on $23SiO_2$-CLD-4A at 65 ppm (0.44 mmol/g), which indicates $H_2S$ molecules are not blocked in $23SiO_2$-CLD-4A. The results suggest that the CLD modified 4A zeolite samples are also effective size-selective sorbents for $H_2S$ removal from natural gas.

Adsorption of $CO_2$ from flue/postcombustion gas (predominantly $CO_2/N_2$ separation) is an important aspect of carbon capture and storage (CCS). The same sorbent for $CO_2/CH_4$ separation was used in $CO_2/N_2$ separation. Figure 6 shows the pure $CO_2$ and $N_2$ isotherms of 4A zeolite and $27SiO_2$-CLD-4A. The amount of $CO_2$ adsorbed (at 760 Torr) on $27SiO_2$-CLD-4A decreased to 70% of the 4A zeolite capacity (4.1 mmol/g). The $N_2$ capacity of the $27SiO_2$-CLD-4A sample was 0.06 mmol/g, which is 15% of the $N_2$ capacity of 4A zeolite (0.4 mmol/g). The drastic decrease of the $N_2$ capacity conclusively demonstrates that most pores of 4A zeolite were reduced to a size smaller than the kinetic diameter of $N_2$ molecules (0.36 nm) and remained larger than the kinetic diameter of $CO_2$ (0.33 nm). Flue gas has a composition of approximately 80%


DOI: 10.1021/acssuschemeng.8b05339
ACS Sustainable Chem. Eng. 2019, 7, 3301–3308

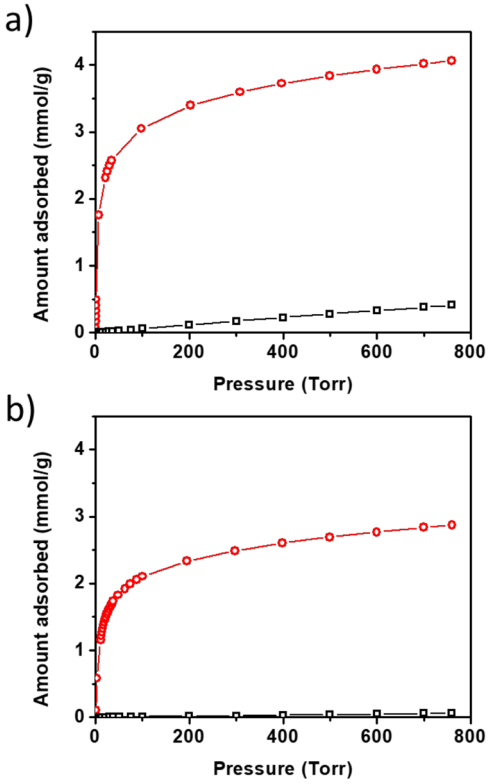


**Figure 6.** $CO_2$ (○) and $N_2$ (□) isotherms on (a) 4A zeolite and (b) $27SiO_2$-CLD-4A at 298 K.

of $N_2$ and 15% of $CO_2$. With regards to the conditions compatible with flue gas, the corresponding pure-component selectivity of $CO_2$ over $N_2$ for $27SiO_2$-CLD-4A sample was 44 (calculated by using $CO_2$ capacity at 0.15 atm and $N_2$ capacity at 0.8 atm), about 5 times the $CO_2$ over $N_2$ selectivity for 4A zeolite. To the best of our knowledge, this is the highest selectivity reported for nonamine sorbents.

The $O_2$ content in air (21%) is lower than $N_2$ content (78%), and so, less energy is required to separate air by using an $O_2$ selective sorbent. The kinetic diameter of $O_2$ is 0.35 nm, which is 0.01 nm smaller than $N_2$ (0.36 nm). It is indeed possible to create an $O_2$ selective sorbent if the effective pore aperture of the sorbent is large enough to allow $O_2$ molecules to pass through and small enough to exclude $N_2$ molecules. In this respect, we investigated the effect of the deposited amount of $SiO_2$ on the selectivity of air separation over 4A zeolite. The $N_2$, $O_2$ and Ar adsorption isotherms on 4A zeolite and CLD-modified 4A samples are displayed in Figure 7. It shows that nitrogen has higher selectivity over oxygen and argon on 4A zeolite. After depositing 16 wt % $SiO_2$ on 4A zeolite, the majority of nitrogen molecules are restricted from entering 4A zeolite pores. The nitrogen adsorption capacity decreased from 0.4 to 0.16 mmol/g, slightly higher than the amount of oxygen adsorbed on $16SiO_2$-CLD-4A sample. Increasing the $SiO_2$ deposition amount to 23 wt % further decreased the nitrogen adsorption capacity to 0.09 mmol/g, below the capacity of oxygen. This shows clear and significant $O_2/N_2$ selectivity. On the $27SiO_2$-CLD-4A sample, the sorbent remained oxygen selective while the adsorption capacities of both nitrogen and oxygen decreased. It is worth noting that the nitrogen adsorption capacity decreased with the increasing amount of $SiO_2$ deposited, whereas the oxygen adsorption capacity remained almost unaffected until 27 wt % $SiO_2$ was deposited. This demonstrates that the size-selective separation ability of the CLD-modified 4A zeolites can be controlled by changing the deposited amount of $SiO_2$. As the $SiO_2$ amount increased, more pores obtained the aperture size to exclude $N_2$ molecules, reducing the $N_2$ adsorptive capacity. Further increasing the $SiO_2$ amount resulted in the reduction of some pore apertures smaller than the size of $O_2$ molecules, jeopardizing the $O_2$ adsorptive capacity.

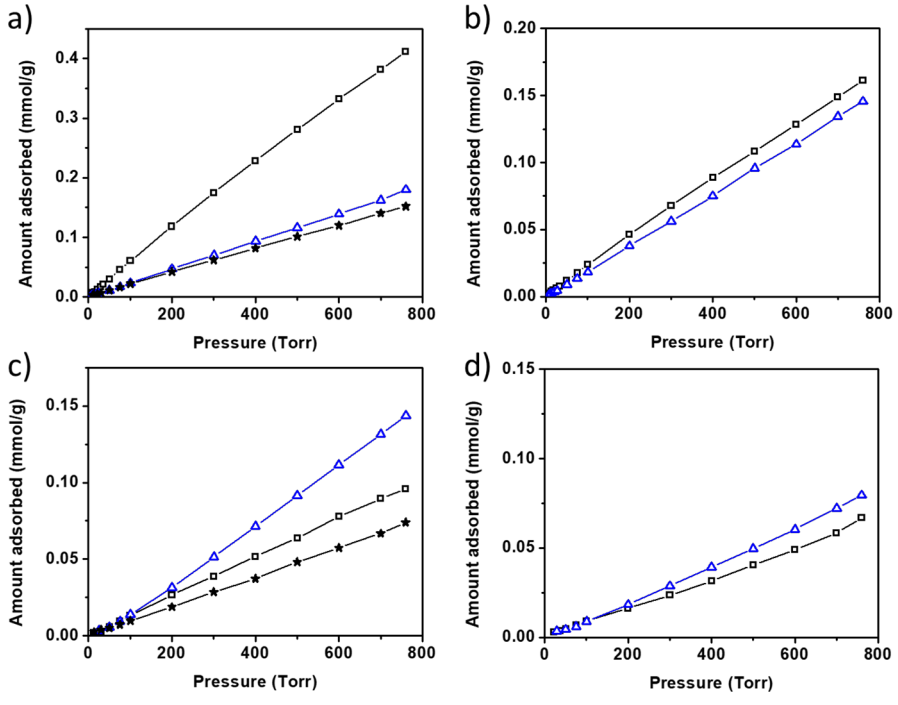


**Figure 7.** $O_2$ (△), $N_2$ (□) and Ar (*) isotherms on (a) 4A zeolite, (b) $16SiO_2$-CLD-4A, (c) $23SiO_2$-CLD-4A and (d) $27SiO_2$-CLD-4A at 298 K.



DOI: 10.1021/acssuschemeng.8b05339
ACS Sustainable Chem. Eng. 2019, 7, 3301−3308

The production of high-purity oxygen requires the separation of oxygen and argon. The oxygen produced from air separation by PSA process has a 95% purity limit due to the presence of argon. Since oxygen and argon are comparable in size, boiling points and isosteric heats of adsorption on most sorbents, it is difficult to separate oxygen and argon at ambient temperature. Currently, $O_2$/Ar separation is conducted under cryogenic temperatures in industrial processes, which is highly energy intensive. Therefore, the development of a selective sorbent for $O_2$/Ar at ambient temperature is of practical significance. As shown in Figure 7, the 23$SiO_2$-CLD-4A sample is the best sorbent for $O_2$ selective air separation with an $O_2$/$N_2$ pure-component selectivity of 1.6. The argon adsorption isotherms on 4A zeolite and 23$SiO_2$−-CLD-A are obtained at 298 K. The argon adsorption capacity decreased to 0.07 mmol/g from the initial value of 0.15 mmol/g for 4A zeolite, while the oxygen adsorption capacity only changed by 0.03 mmol/g. This is noteworthy because the kinetic diameter of argon molecular is smaller than oxygen. Thus, the decrease of argon capacity should not be larger than oxygen. Based on the work of Kuznicki et al.,[39] the larger reduction in argon capacity when compared to oxygen can be attributed to the pores being exposed to the smaller cross section of the oxygen molecule because it approaches along the diatomic axis. Argon, however, acts as a solid sphere and does not have this favored orientation. Webley at al. also observed a improved $O_2$/Ar pure-component selectivity on potassium exchanged CHA zeolite due to the partial pore blockage,[40] which is in agreement with our results. Calculated from the adsorption capacities at 760 Torr, the pure-component selectivity of $O_2$ over Ar for 23$SiO_2$-CLD-4A sample was about 2, making the sorbent applicable for $O_2$/Ar separation by PSA process.

It is commonly believed or assumed that silylation by CLD is achieved by reaction between the deposition agent and the zeolite surface hydroxyl groups (silanol groups and bridging hydroxyl groups). Subsequently, the deposited coating is converted to silica layer by calcination.

The possible reactions are listed below:

$$\text{Zeolite}-\text{OH} + \text{SiCl}_4 \rightarrow \text{Zeolite}-\text{O}-\text{SiCl}_3 + \text{HCl} \quad (2)$$

$$\text{Zeolite}-\text{O}-\text{SiCl}_3 + 3\text{H}_2\text{O} \rightarrow \text{Zeolite}-\text{O}-\text{Si(OH)}_3 + 3\text{HCl} \quad (3)$$

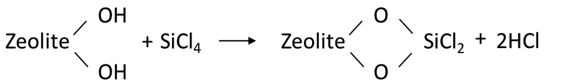


(4)

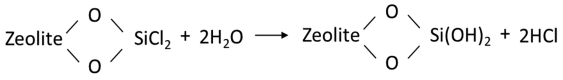


(5)

To further understand the mechanism of CLD modification for 4A zeolite, we calcined 4A zeolite at 823 K (for dehydroxylation) and performed the CLD process immediately after calcination. The amount of the deposition agent and CLD modification procedure used for the calcined 4A zeolite is the same as the 27$SiO_2$-CLD-4A. The sample is referred to as 27$SiO_2$-cal-4A. The CLD modification on calcined 4A zeolite is not effective. As shown in Figure 8, the methane capacity of 27$SiO_2$-cal-4A was 0.5 mmol/g, much higher than the methane capacity of 27$SiO_2$-CLD-4A sample (0.04 mmol/g). The amount of hydroxyl groups on 4A zeolite and calcined 4A

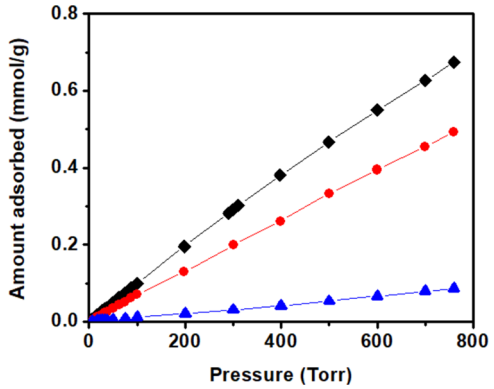


**Figure 8.** Methane adsorption isotherms on 4A zeolite (◆), 27$SiO_2$-cal-4A (●) and 27$SiO_2$-water-4A (▲).

zeolite samples were analyzed by TGA in a helium flow (Figure 9). The TGA thermogram of 4A zeolite showed a total of

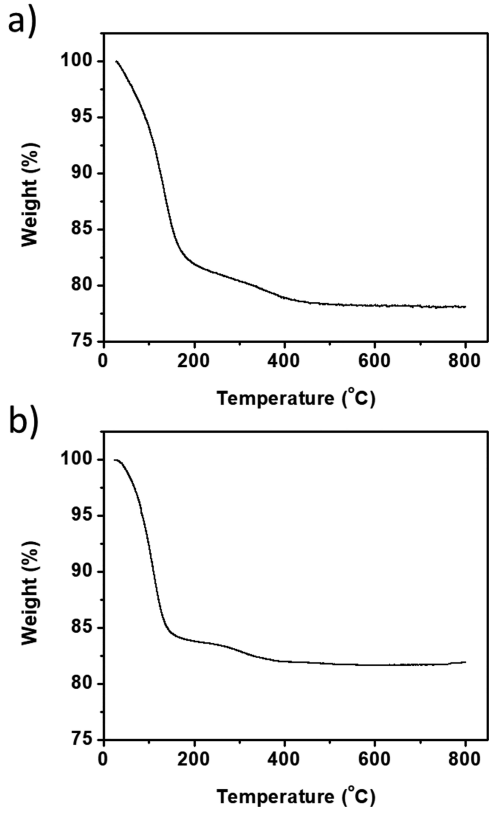


**Figure 9.** TGA thermogram of (a) 4A zeolite (b) calcined 4A zeolite in a helium atmosphere.

21.9% weight loss consisting of two step losses at temperatures below 150 °C and between 150 and 550 °C. According to results from previous studies,[20,41] the steep weight loss of 14.9% below 150 °C was attributed to the removal of adsorbed water and the weight loss of 7.0% above 150 °C was attributed to the dehydroxylation by condensation of hydroxyl groups. For the calcined 4A zeolite sample, the TGA thermogram showed a similar two step losses curve with a total weight loss of 18.3%. The weight loss of 15.5% below 150 °C and the weight loss of 2.8% above 150 °C were assigned to the removal of water and hydroxyl group condensation, respectively. The TGA results confirmed that significantly fewer hydroxyl groups



DOI: 10.1021/acssuschemeng.8b05339
ACS Sustainable Chem. Eng. 2019, 7, 3301−3308

were preserved on 4A zeolite after calcination. The less effective pore aperture reduction was clearly due to the lower amount of hydroxyl groups on calcined 4A zeolite. According to Wang and Wunder, the number of silanol groups can be increased by treating silica in water.[42] In this respect, we soaked calcined 4A zeolite in DI water for 30 min at ambient temperature, then dried the sample at 373 K for 3 h before the CLD modification process. The same deposition amount and procedures were used as 27$SiO_2$-cal-4A and 27$SiO_2$-CLD-4A. This sample is referred to as 27$SiO_2$-water-4A. The methane isotherm of 27$SiO_2$-water-4A given in Figure 8 showed a capacity of 0.08 mmol/g, indicating the effective pore aperture size reduction after CLD modification. These results confirmed the hypothesis that hydroxyl groups are essential for CLD and pore aperture reduction by CLD process.

As mentioned, moisture in the feed is removed by using a layer of desiccant (typically silica or alumina) at the inlet of the adsorber bed in commercial PSA processes, e.g., air separation and hydrogen purification using zeolites. The CLD-4A sorbent has a core−shell structure, with a shell of silica. Investigation on the possibility of using the CLD silica shell as a guard layer against moisture is in progress.

## CONCLUSIONS

We employed the CLD process on 4A zeolite to prepare a size-selective sorbent for the separation of molecules with 0.01 nm size differences. It is shown that the pore aperture sizes can be optimized by changing the amount of silica deposited on the 4A zeolite surface for a targeted separation of small molecules. The resulting CLD modified 4A zeolite samples achieved high pure-component selectivities of 76 for $CO_2/CH_4$ separation and 44 for $CO_2/N_2$ separation. The optimized CLD modified 4A zeolite for oxygen-selective air separation possessed remarkable selectivities of 1.6 for $O_2/N_2$ separation and 2 for $O_2$/Ar separation. The CLD modified 4A zeolite samples are also promising sorbents for selective removal of $H_2S$ from methane. The $N_2$ adsorption−desorption isotherms at 77 K showed the silica layer deposited on the CLD modified 4A zeolites contained mesopores. Moreover, study on the CLD mechanism showed that hydroxyl groups on 4A zeolite surface were essential for CLD and pore aperture modification by the CLD process.

## ASSOCIATED CONTENT

### Supporting Information

The Supporting Information is available free of charge on the ACS Publications website at DOI: 10.1021/acssuschemeng.8b05339.

Experimental results including rates of adsorption and heats of adsorption (PDF)

## AUTHOR INFORMATION


### Corresponding Author

*R. T. Yang. Email: yang@umich.edu.

### ORCID

Yiren Wang: 0000-0002-9935-0806

Ralph T. Yang: 0000-0002-5367-9550

### Present Address

Y.W.: 3074 H.H. Dow, 2300 Hayward Street, Ann Arbor, MI 48109-2136, USA


### Notes

The authors declare no competing financial interest.

## ACKNOWLEDGMENTS

Funding from China Scholarship Council, University of Michigan BlueSky Global CO2 Initiative and NSF CBET-1826621 is gratefully acknowledged.

## REFERENCES


(1) Yang, R. T. *Adsorbents: Fundamentals and Applications*; Wiley: New York, 2003; DOI: 10.1002/047144409X.

(2) Breck, D. W. *Zeolite molecular sieves: structure, chemistry, and use*; Wiley: New York, 1973.

(3) Niwa, M.; Kato, S.; Hattori, T.; Murakami, Y. Fine control of the pore-opening size of the zeolite mordenite by chemical vapour deposition of silicon alkoxide. *J. Chem. Soc., Faraday Trans. 1* **1984**, *80* (11), 3135−3145.

(4) Kuznicki, S. M.; Bell, V. A.; Nair, S.; Hillhouse, H. W.; Jacubinas, R. M.; Braunbarth, C. M.; Toby, B. H.; Tsapatsis, M. A titanosilicate molecular sieve with adjustable pores for size-selective adsorption of molecules. *Nature* **2001**, *412*, 720.

(5) Song, Z.; Huang, Y.; Xu, W. L.; Wang, L.; Bao, Y.; Li, S.; Yu, M. Continuously Adjustable, Molecular-Sieving "Gate" on 5A Zeolite for Distinguishing Small Organic Molecules by Size. *Sci. Rep.* **2015**, *5*, 13981.

(6) Yue, Y. H.; Tang, Y.; Liu, Y.; Gao, Z. Chemical Liquid Deposition Zeolites with Controlled Pore-Opening Size and Shape-Selective Separation of Isomers. *Ind. Eng. Chem. Res.* **1996**, *35* (2), 430−433.

(7) Zhao, Y. W.; Shen, B. X.; Sun, H. Chemical Liquid Deposition Modified ZSM-5 Zeolite for Adsorption Removal of Dimethyl Disulfide. *Ind. Eng. Chem. Res.* **2016**, *55* (22), 6475−6480.

(8) Wanigarathna, D. K. J. A.; Liu, B.; Gao, J. Adsorption separation of R134a, R125, and R143a fluorocarbon mixtures using 13X and surface modified 5A zeolites. *AIChE J.* **2018**, *64* (2), 640−648.

(9) Li, J. Y.; Corma, A.; Yu, J. H. Synthesis of new zeolite structures. *Chem. Soc. Rev.* **2015**, *44* (20), 7112−7127.

(10) Morris, R. E.; Čejka, J. Exploiting chemically selective weakness in solids as a route to new porous materials. *Nat. Chem.* **2015**, *7*, 381.

(11) Liang, X.; Yu, M.; Li, J.; Jiang, Y. B.; Weimer, A. W. Ultra-thin microporous−mesoporous metal oxide films prepared by molecular layer deposition (MLD). *Chem. Commun.* **2009**, *0* (46), 7140−7142.

(12) Zheng, S.; Heydenrych, H. R.; Jentys, A.; Lercher, J. A. Influence of Surface Modification on the Acid Site Distribution of HZSM-5. *J. Phys. Chem. B* **2002**, *106* (37), 9552−9558.

(13) Ryckebosch, E.; Drouillon, M.; Vervaeren, H. Techniques for transformation of biogas to biomethane. *Biomass Bioenergy* **2011**, *35* (5), 1633−1645.

(14) Shah, M. S.; Tsapatsis, M.; Siepmann, J. I. Hydrogen Sulfide Capture: From Absorption in Polar Liquids to Oxide, Zeolite, and Metal−Organic Framework Adsorbents and Membranes. *Chem. Rev.* **2017**, *117* (14), 9755−9803.

(15) Choi, S.; Drese, J. H.; Jones, C. W. Adsorbent Materials for Carbon Dioxide Capture from Large Anthropogenic Point Sources. *ChemSusChem* **2009**, *2* (9), 796−854.

(16) Webley, P. A. Adsorption technology for CO2 separation and capture: a perspective. *Adsorption* **2014**, *20* (2), 225−231.

(17) Cavenati, S.; Grande, C. A.; Rodrigues, A. E. Upgrade of Methane from Landfill Gas by Pressure Swing Adsorption. *Energy Fuels* **2005**, *19* (6), 2545−2555.

(18) Harlick, P. J. E.; Tezel, F. H. An experimental adsorbent screening study for CO2 removal from N2. *Microporous Mesoporous Mater.* **2004**, *76* (1), 71−79.

(19) Darunte, L. A.; Walton, K. S.; Sholl, D. S.; Jones, C. W. CO2 capture via adsorption in amine-functionalized sorbents. *Curr. Opin. Chem. Eng.* **2016**, *12*, 82−90.

(20) Wang, L.; Yang, R. T. Increasing Selective CO2 Adsorption on Amine-Grafted SBA-15 by Increasing Silanol Density. *J. Phys. Chem. C* **2011**, *115* (43), 21264−21272.
(21) Choi, S.; Drese, J. H.; Eisenberger, P. M.; Jones, C. W. Application of Amine-Tethered Solid Sorbents for Direct CO2 Capture from the Ambient Air. *Environ. Sci. Technol.* **2011**, *45* (6), 2420−2427.
(22) Vilarrasa-García, E.; Cecilia, J. A.; Bastos-Neto, M.; Cavalcante, C. L.; Azevedo, D. C. S.; Rodriguez-Castellón, E. CO2/CH4 adsorption separation process using pore expanded mesoporous silicas functionalizated by APTES grafting. *Adsorption* **2015**, *21* (8), 565−575.
(23) Xu, X.; Song, C.; Andresen, J. M.; Miller, B. G.; Scaroni, A. W. Novel Polyethylenimine-Modified Mesoporous Molecular Sieve of MCM-41 Type as High-Capacity Adsorbent for CO2 Capture. *Energy Fuels* **2002**, *16* (6), 1463−1469.
(24) Ma, X.; Wang, X.; Song, C. Molecular Basket" Sorbents for Separation of CO2 and H2S from Various Gas Streams. *J. Am. Chem. Soc.* **2009**, *131* (16), 5777−5783.
(25) Bezerra, D. P.; Silva, F. W. M. d.; Moura, P. A. S. d.; Sousa, A. G. S.; Vieira, R. S.; Rodriguez-Castellon, E.; Azevedo, D. C. S. CO2 adsorption in amine-grafted zeolite 13X. *Appl. Surf. Sci.* **2014**, *314*, 314−321.
(26) Moura, P. A. S.; Bezerra, D. P.; Vilarrasa-Garcia, E.; Bastos-Neto, M.; Azevedo, D. C. S. Adsorption equilibria of CO2 and CH4 in cation-exchanged zeolites 13X. *Adsorption* **2016**, *22* (1), 71−80.
(27) Shang, J.; Li, G.; Singh, R.; Gu, Q.; Nairn, K. M.; Bastow, T. J.; Medhekar, N.; Doherty, C. M.; Hill, A. J.; Liu, J. Z.; Webley, P. A. Discriminative Separation of Gases by a "Molecular Trapdoor" Mechanism in Chabazite Zeolites. *J. Am. Chem. Soc.* **2012**, *134* (46), 19246−19253.
(28) Kennedy, D. A.; Tezel, F. H. Cation exchange modification of clinoptilolite − Screening analysis for potential equilibrium and kinetic adsorption separations involving methane, nitrogen, and carbon dioxide. *Microporous Mesoporous Mater.* **2018**, *262*, 235−250.
(29) Wu, Z.; Webley, P. A.; Zhao, D. Post-enrichment of nitrogen in soft-templated ordered mesoporous carbon materials for highly efficient phenol removal and CO2 capture. *J. Mater. Chem.* **2012**, *22* (22), 11379−11389.
(30) Bezerra, D. P.; Oliveira, R. S.; Vieira, R. S.; Cavalcante, C. L.; Azevedo, D. C. S. Adsorption of CO2 on nitrogen-enriched activated carbon and zeolite 13X. *Adsorption* **2011**, *17* (1), 235−246.
(31) Vilarrasa-García, E.; Cecilia, J. A.; Bastos-Neto, M.; Cavalcante, C. L.; Azevedo, D. C. S.; Rodríguez-Castellón, E. Microwave-assisted nitric acid treatment of sepiolite and functionalization with polyethylenimine applied to CO2 capture and CO2/N2 separation. *Appl. Surf. Sci.* **2017**, *410*, 315−325.
(32) Cavenati, S.; Grande, C. A.; Rodrigues, A. E.; Kiener, C.; Müller, U. Metal Organic Framework Adsorbent for Biogas Upgrading. *Ind. Eng. Chem. Res.* **2008**, *47* (16), 6333−6335.
(33) Jasuja, H.; Walton, K. S. Experimental Study of CO2, CH4, and Water Vapor Adsorption on a Dimethyl-Functionalized UiO-66 Framework. *J. Phys. Chem. C* **2013**, *117* (14), 7062−7068.
(34) Karra, J. R.; Grabicka, B. E.; Huang, Y. G.; Walton, K. S. Adsorption study of CO2, CH4, N2, and H2O on an interwoven copper carboxylate metal−organic framework (MOF-14). *J. Colloid Interface Sci.* **2013**, *392*, 331−336.
(35) Figueroa, J. D.; Fout, T.; Plasynski, S.; McIlvried, H.; Srivastava, R. D. Advances in CO2 capture technology—The U.S. Department of Energy's Carbon Sequestration Program. *Int. J. Greenhouse Gas Control* **2008**, *2* (1), 9−20.
(36) Berlier, K.; Frère, M. Adsorption of CO2 on Microporous Materials. 1. On Activated Carbon and Silica Gel. *J. Chem. Eng. Data* **1997**, *42* (3), 533−537.
(37) Thommes, M.; Kaneko, K.; Neimark, A. V.; Olivier, J. P.; Rodriguez-Reinoso, F.; Rouquerol, J.; Sing, K. S. W. Physisorption of gases, with special reference to the evaluation of surface area and pore size distribution (IUPAC Technical Report). *Pure Appl. Chem.* **2015**, *87*, 1051−1069.
(38) Huang, H. Y.; Yang, R. T.; Chinn, D.; Munson, C. L. Amine-Grafted MCM-48 and Silica Xerogel as Superior Sorbents for Acidic Gas Removal from Natural Gas. *Ind. Eng. Chem. Res.* **2003**, *42* (12), 2427−2433.
(39) Ansón, A.; Kuznicki, S. M.; Kuznicki, T.; Dunn, B. C.; Eyring, E. M.; Hunter, D. B. Separation of Argon and Oxygen by Adsorption on a Titanosilicate Molecular Sieve. *Sep. Sci. Technol.* **2009**, *44* (7), 1604−1620.
(40) Singh, R. K.; Webley, P. Adsorption of N2, O2, and Ar in Potassium Chabazite. *Adsorption* **2005**, *11* (1), 173−177.
(41) Ward, J. W. The nature of active sites on zeolites: III. The alkali and alkaline earth ion-exchanged forms. *J. Catal.* **1968**, *10* (1), 34−46.
(42) Wang, R.; Wunder, S. L. Effects of Silanol Density, Distribution, and Hydration State of Fumed Silica on the Formation of Self-Assembled Monolayers of n-Octadecyltrichlorosilane. *Langmuir* **2000**, *16* (11), 5008−5016.


DOI: 10.1021/acssuschemeng.8b05339
*ACS Sustainable Chem. Eng.* 2019, 7, 3301−3308